Electronic States and Optical Properties in Cubic Ice*

G. Pastori Parravicini and L. Resca

Istituto di Fisica, Università di Pisa, and Gruppo Nazionale di Struttura della Materia del Consiglio Nazionale delle Ricerche, Pisa, Italy

(Received 20 October 1972)

The electronic states of completely polarized cubic ice are studied using as an expansion set the Bloch sums formed with water molecular orbitals. A complete symmetry analysis appropriate for the nonsymmorphic group of cubic ice is given for a simplified model. The band structure of cubic ice is obtained at high-symmetry points and high-symmetry lines of the Brillouin zone. The calculated energy gap of 7.8 eV is in good agreement with experimental data and corresponds to a critical point of type M_0 at $\vec{k} = 0$. The critical points of type M_1 occurring at the point L of the Brillouin zone are interpreted as responsible for the strong peak in the ultraviolet optical constants at 8.7 eV. The broad absorption band at higher energy (≈ 15 eV) is interpreted as due to transitions from valence bands derived from lone-pair orbitals to the lowest excited bands.

I. INTRODUCTION

Numerous theoretical and experimental studies on the physical properties of ice have been made in the past few years. Recent experimental and theoretical work is reviewed in Refs. 1 and 2. In particular, the optical constants of ice have been studied by a number of authors both in the infrared region[3] and in the ultraviolet region[4] near the fundamental absorption edge. The investigation of the optical constants has been extended up to about 25 eV by means of electron-energy-loss techniques.[5] The use of synchrotron radiation as a light source[6] makes it possible to extend even further the investigation, and some preliminary experiments have already been attempted.[7] The knowledge of the band structure of ice crystals is basic for an understanding of the optical properties above the energy gap and constitutes the main purpose of this paper.

Ice can crystallize in a large number of structures. Any ice crystal is formed by water molecules located in such a way to satisfy the hypotheses of Pauling[8] that (i) the molecules of H_2O are intact in ice and (ii) along the direction O-O there is one and only one hydrogen atom, closer to one or the other of the two oxygen atoms. Thus in a given ice structure the oxygen positions are fixed, while the hydrogen positions are random, provided they satisfy the hypotheses of Pauling.

In cubic ice (CI) the sublattice of the oxygen atoms is the same as the fcc diamond structure. Every oxygen is surrounded by four nearest-neighbor oxygens in a tetrahedral configuration and there are two oxygens in the unit cell. In the oxygen sublattice the site symmetry around an oxygen position is T_d, the point group is $O_h = T_d x(E, I)$, and the space group is not symmorphic because the inversion symmetry I is associated with the fractional translation which exchanges the two oxygens in the unit cell. If we now consider the fact that

the hydrogen atoms make two of the four O-O directions different from the other two we immediately have that the maximum site symmetry of cubic ice crystals is the subgroup C_{2v} of T_d and its maximum point-group symmetry is the subgroup C_{4v} of O_h, with a nonsymmorphic space group.

In CI two nearest-neighbor water molecules can take three different relative orientations, because of the tetrahedral coordination of the oxygen atoms and the random distribution of the hydrogen atoms. According to the statistical model of Pauling,[8] each of these three relative orientations occurs with the same probability. In order to construct a meaningful and simple model for obtaining the band structure of ice, we take advantage of the fact that the general electron density distribution for the water molecule is practically spherically symmetric around the oxygen,[9] which is the typical case for the O-H interaction. In such a physical situation we expect that the overlap between two electron clouds centered on two nearest-neighbor molecules is approximately the same whatever relative orientation of the two molecules is considered. Also the overlap between the electron cloud of a given molecule and the electron cloud of its nearest-neighbor molecule multiplied by the molecular potential (which is not spherically symmetric because of the proton contributions) does not depend on the three possible relative orientations. The overlap integrals and potential integrals just described determine the electronic states in ice; since they are independent from the relative molecular orientations, we assume, for convenience, that the two molecules in the unit cell are lined up with parallel axes. We will further discuss quantitatively this assumption in Sec. IV.

In a previous work,[10] we noticed that the particular relative orientation in which the axes of the two molecules per unit cell are lined up preserves fcc translational symmetry and gives a periodic structure, which we call cubic-ice model structure

(CIMS), to which the powerful methods of elec-
tronic-state calculations can be applied. The CIMS
has a nonsymmorphic space group with point group
C_{4v} and constitutes the maximum-symmetry model
for CI. We will now study the electronic states
using the molecular tight-binding approach along
lines similar to those briefly outlined in our pre-
vious work.[10] Incidentally, we notice that CIMS
should occur in the ferroelectric phase of cubic
ice[11] or upon application of a sufficiently strong
electric field while crystals are being made, as
suggested by Onaka[12]; however, these two points
have not yet been confirmed.

In Sec. II the symmetry analysis of the cubic-ice
model structure is performed by applying proce-
dures appropriate for nonsymmorphic groups. In
Sec. III the procedure adopted for calculation of
the electronic states is given. Section IV contains
the results and the interpretation of the first ab-
sorption bands in the ultraviolet region. Section V
contains the conclusions.

II. SYMMETRY ANALYSIS OF CUBIC-ICE MODEL STRUCTURE

The symmetry group of H_2O molecule is C_{2v}.
This group consists of the identity E, the rotation
C_2 by π around the line bisecting the H-O-H angle,
the reflection σ_v in the plane containing the twofold
axis and normal to the plane of the molecule, the
reflection σ_h (often indicated in the literature with
σ_v') in the plane of the molecule. In Table I the ir-
reducible representations of the group C_{2v} are re-
ported for convenience. We see that basis func-
tions of type A_1 (A_2) are even (odd) under both re-
flections σ_v and σ_h, while basis functions of type
B_1 (B_2) are even (odd) under σ_v (σ_h) and odd (even)
under σ_h (σ_v).

The CIMS described in the Introduction is sche-
matically shown in Fig. 1, where for simplicity
only the four hydrogens in the unit cell have been
indicated. The other hydrogens are located in such
a way to form water molecules with the twofold axis
parallel to the x axis. The translational symmetry
of CIMS is fcc, with fundamental vectors

$$\vec{\tau}_1 = \tfrac{1}{2} a_0(0,1,1) \ ,$$

$$\vec{\tau}_2 = \tfrac{1}{2} a_0(1,0,1) \ , \tag{2.1}$$

TABLE I. Irreducible representations of the symmetry group C_{2v}.

Group C_{2v}	E	C_2	σ_v	σ_h
A_1	1	1	1	1
A_2	1	1	-1	-1
B_1	1	-1	1	-1
B_2	1	-1	-1	1
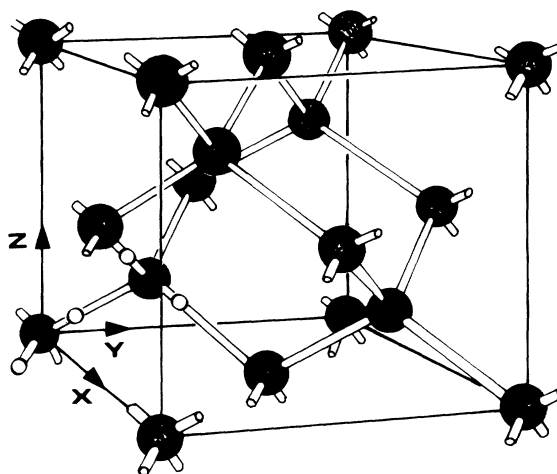
FIG. 1. Schematic representations of the cubic-ice
model structure. The oxygen positions are represented
with black circles. The hydrogens of the two molecules
per unit cell are also shown.

$$\vec{\tau}_3 = \tfrac{1}{2} a_0(1,1,0) \ ,$$

with $a_0 = 6.35$ Å at the temperature of 138 °K. With
the choice of axes of Fig. 1, the two oxygens per
unit cell are in the positions

$$\vec{\delta}_{1O} = (0,0,0) \ ,$$

$$\vec{\delta}_{2O} = \tfrac{1}{4} a_0(1,1,1) \ . \tag{2.2}$$

The four hydrogens are in the positions

$$\vec{\delta}_{1H} = \tfrac{1}{8} a_0(\beta, \beta, \beta) \ ,$$

$$\vec{\delta}_{2H} = \tfrac{1}{8} a_0(\beta, -\beta, -\beta) \ ,$$

$$\vec{\delta}_{3H} = \tfrac{1}{8} a_0(\beta+2, -\beta+2, \beta+2) \ , \tag{2.3}$$

$$\vec{\delta}_{4H} = \tfrac{1}{8} a_0(\beta+2, \beta+2, -\beta+2) \ ,$$

where $\beta = 0.7$ corresponds to an O-H separation of
1.83 a.u. as in free water[13] and to a H-O separa-
tion of the hydrogen bond of 3.36 a.u. It is im-
mediately noted that

$$\left| \vec{\delta}_{1H} - \vec{\delta}_{1O} \right| = \left| \vec{\delta}_{2H} - \vec{\delta}_{1O} \right|$$

$$= \left| \vec{\delta}_{3H} - \vec{\delta}_{2O} \right| = \left| \vec{\delta}_{4H} - \vec{\delta}_{2O} \right| \ ,$$

so that the first water molecule in the unit cell is
constituted by the oxygen $\vec{\delta}_{1O}$ and the hydrogens $\vec{\delta}_{1H}$
and $\vec{\delta}_{2H}$, while the second molecule in the unit cell
is constituted by the oxygen $\vec{\delta}_{2O}$ and the hydrogens
$\vec{\delta}_{3H}$ and $\vec{\delta}_{4H}$. The smallest H-H distance is

$$\left| \vec{\delta}_{3H} - \vec{\delta}_{1H} \right| = \left| \vec{\delta}_{4H} - \vec{\delta}_{1H} \right| = \left| \vec{\delta}_{3H} - \vec{\tau}_2 - \vec{\delta}_{1H} \right|$$

$$= \left| \vec{\delta}_{4H} - \vec{\tau}_3 - \vec{\delta}_{1H} \right| = 4.34 \text{ a.u.} \ ;$$

the next smallest H-H distance is $\left| \vec{\delta}_{2H} + \vec{\tau}_1 - \vec{\delta}_{1H} \right|$
$= 5.52$ a.u. The smallest O-O distance is

TABLE II. Symmetry operations of the cubic-ice model structure. The symmetry operations are indicated using standard notations. For instance, $I\delta_{2y,-z}$ indicates the rotation by $2\pi/2$ along the axis, whose director cosines are in the ratio $0:1:\bar{1}$, followed by inversion. For convenience, the coordinate transformations are also given.

Symmetry operations	Coordinate transformations			Symmetry operations	Coordinate transformations		
$\{E\mid 0\}$	x	y	z	$\{\delta_{4x}\mid\vec{f}\}$	$x+\tfrac{1}{4}a_0$	$z+\tfrac{1}{4}a_0$	$\bar{y}+\tfrac{1}{4}a_0$
$\{\delta_{2x}\mid 0\}$	x	$\bar{y}$	$\bar{z}$	$\{\delta_{4x}^{-1}\mid\vec{f}\}$	$x+\tfrac{1}{4}a_0$	$\bar{z}+\tfrac{1}{4}a_0$	$y+\tfrac{1}{4}a_0$
$\{I\delta_{2yz}\mid 0\}$	x	$\bar{z}$	$\bar{y}$	$\{I\delta_{2y}\mid\vec{f}\}$	$x+\tfrac{1}{4}a_0$	$\bar{y}+\tfrac{1}{4}a_0$	$z+\tfrac{1}{4}a_0$
$\{I\delta_{2y,-z}\mid 0\}$	x	z	y	$\{I\delta_{2z}\mid\vec{f}\}$	$x+\tfrac{1}{4}a_0$	$y+\tfrac{1}{4}a_0$	$\bar{z}+\tfrac{1}{4}a_0$

$$\left|\vec{\delta}_{20}-\vec{\delta}_{10}\right|=\left|\vec{\delta}_{20}-\vec{\tau}_1-\vec{\delta}_{10}\right|=\left|\vec{\delta}_{20}-\vec{\tau}_2-\vec{\delta}_{10}\right|$$

$$=\left|\vec{\delta}_{20}-\vec{\tau}_3-\vec{\delta}_{10}\right|=5.20 \text{ a. u.}$$

Because of Eq. (2.1), the Brillouin zone corresponding to CIMS is the usual truncated octahedron[14] shown in Fig. 2. Since the point-symmetry group C_{4v} of CIMS is not a cubic group, the symmetry properties of the energy as a function of $\vec{k}$ in the Brillouin zone are completely different from those of cubic crystals with fcc structure. In particular we notice that the line k_x is not equivalent to the lines k_y, k_z in CIMS. For convenience, the symmetry operations of the group C_{4v} are indicated in Table II. The space group is not symmorphic since half of the symmetry operations of C_{4v} are associated with the fractional translation $\vec{f}=\tfrac{1}{4}a_0$ $(1,1,1)=\vec{\delta}_{20}-\vec{\delta}_{10}$, which exchanges the two molecules among themselves.

At the center of the Brillouin zone and along the line k_x the crystal states are classified according to the irreducible representations of the group C_{4v}. The irreducible representations at Δ, p, and X are reported in Table III. We notice explicitly the importance of the phase factor $e^{-i\pi p/2}$, whose appearance is due to the fact that the group is not symmorphic.[14] Because of this phase factor the
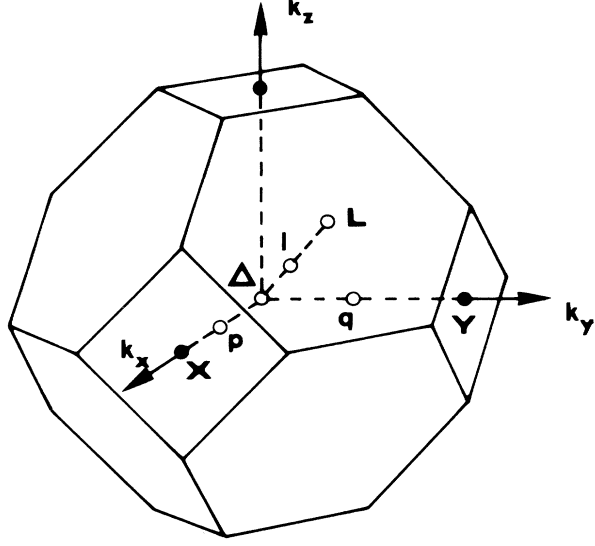
FIG. 2. Brillouin zone, symmetry points, and symmetry lines of the cubic-ice model structure.

representations X_1, X_2' and X_1', X_2 are degenerate by time-reversal symmetry, as can be seen by applying Herring's test.[15] All crystal states are thus doubly degenerate at the point X.

Along the line k_y, that is equivalent to k_z but not to k_x, the symmetry operations are $\{E\mid 0\}$ and $\{I\delta_{2z}\mid\vec{f}\}$, and we indicate with q_1 and q_2 the even and the odd representation.

At the point $Y[\vec{k}=(2\pi/a_0)(0,1,0,)]$ the symmetry operations which leave $\vec{k}$ unchanged are $\{E\mid 0\}$, $\{\delta_{2x}\mid 0\}$, $\{I\delta_{2y}\mid\vec{f}\}$, $\{I\delta_{2z}\mid\vec{f}\}$. To obtain in this case the irreducible representations, we notice that for $\vec{k}=(2\pi/a_0)(0,1,0)$ and $\vec{\tau}_\nu=n_1\vec{\tau}_1+n_2\vec{\tau}_2+n_3\vec{\tau}_3$, $e^{i\vec{k}\cdot\vec{\tau}_\nu}\equiv e^{i\pi(n_1+n_3)}$ takes either the value 1 or -1 when the sum n_1+n_3 is even or odd, respectively. We collect all the translations in the two sets, which we indicate by $\{E\mid 0\}$ and $\{E\mid 1\}$ corresponding to the value 1 or -1 of $e^{i\vec{k}\cdot\vec{\tau}_\nu}$. Then we consider a new group whose elements are reported in Table IV and

TABLE III. Irreducible representations at the point Δ, along the line p, and at the point X of the Brillouin zone. The phase factor $e^{-i\pi p/2}$ equals 1 at the point Δ and equals $-i$ at the point X. The representations X_1, X_2' and X_1', X_2 are degenerate by time-reversal symmetry.

Point Δ $\vec{k}=(0,0,0)$	Line p $\vec{k}=(2\pi/a_0)(p,0,0)$	Point X $\vec{k}=(2\pi/a_0)(1,0,0)$	$\{E\mid 0\}$	$\{\delta_{2x}\mid 0\}$	$\{\delta_{4x}\mid\vec{f}\}$ $\{\delta_{4x}^{-1}\mid\vec{f}\}$	$\{I\delta_{2y}\mid\vec{f}\}$ $\{I\delta_{2z}\mid\vec{f}\}$	$\{I\delta_{2yz}\mid 0\}$ $\{I\delta_{2y,-z}\mid 0\}$
Δ_1	p_1	$\Big\{\begin{array}{c} X_1 \end{array}$	1	1	$e^{-i\pi p/2}$	$e^{-i\pi p/2}$	1
Δ_2'	p_2'	X_2'	1	1	$-e^{-i\pi p/2}$	$-e^{-i\pi p/2}$	1
Δ_1'	p_1'	$\Big\{\begin{array}{c} X_1' \end{array}$	1	1	$e^{-i\pi p/2}$	$-e^{-i\pi p/2}$	-1
Δ_2	p_2	X_2	1	1	$-e^{-i\pi p/2}$	$e^{-i\pi p/2}$	-1
Δ_5	p_5	X_5	2	-2	0	0	0

TABLE IV. Irreducible representation at the point Y of the Brillouin zone.

Point Y $\vec{k}=(2\pi/a_0)(0,1,0)$	$\{E\mid 0\}$	$\{E\mid 1\}$	$\{\delta_{2x}\mid 0\}$ $\{\delta_{2x}\mid 1\}$	$\{I\delta_{2y}\mid\vec{t}\}$ $\{I\delta_{2y}\mid\vec{t}+1\}$	$\{I\delta_{2z}\mid\vec{t}\}$ $\{I\delta_{2z}\mid\vec{t}+1\}$
Y_1	2	-2	0	0	0

whose multiplication rule is the inner product of two sets. From all the irreducible representations of the new group one must consider only those appropriate to Bloch functions of vector $\vec{k}$. The two-dimensional irreducible representation so obtained is reported in Table IV. At the point Y all crystal states are thus doubly degenerate.

Along the line l $[\vec{k}=(2\pi/a_0)(l,l,l),\ 0<l<1]$ and at the point L $[\vec{k}=(2\pi/a_0)(1,1,1)]$ the symmetry operations are $\{E\mid 0\}$ and $\{I\delta_{2y,-z}\mid 0\}$, and we indicate with $l_1(L_1)$ and $l_2(L_2)$ the even and the odd representations, respectively.

To complete our symmetry analysis we give in Table V the allowed optical transitions between irreducible representations at high-symmetry points of the Brillouin zone. The allowed optical transitions at the line p and at the point X are the same as in Δ. The allowed optical transitions at the line l and at the point L are the same as in q.

III. CALCULATION OF THE ELECTRONIC STATES

A. Molecular Orbitals of Water

In order to avoid possible confusion let us first clearly define the internal frame of a water molecule as follows: The origin of the internal frame is chosen in O, y_{int} is perpendicular to the water molecule plane, z_{int} lies in the plane of the molecule and bisects the H-O-H concave angle, x_{int} is in the plane of the molecule and is perpendicular to y_{int} and z_{int} (Fig. 3). The molecular orbitals of water have been computed by a number of authors.[16,17] For our purpose, we choose an expansion of molecular orbitals in the so-called minimal set[16] constituted by the Slater-type functions $1s$, $2s$, $2p_x$, $2p_y$, $2p_z$ centered on the oxygen atom, and two $1s$ Slater-type functions centered on the hydrogen atoms. The molecular orbitals are written as
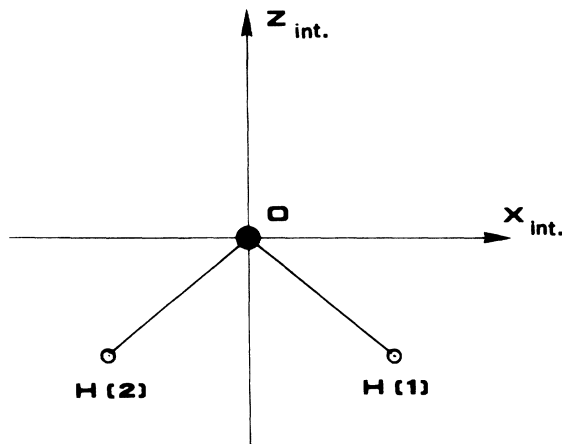
FIG. 3. Internal reference frame for the water molecule.

$$\psi_j(\vec{r})=\sum_{m=1}^{7}a_{jm}\,\varphi_m(\vec{r}-\vec{d}_m)\ ,\qquad(3.1)$$

where the coefficients a_{jm} and the exponents of the Slater-type functions φ_m are obtained from self-consistent calculations for the free molecule. In Table VI we report the coefficients a_{jm}, the exponentials and the centers $\vec{d}_m$ of the Slater-type wave functions φ_m and the corresponding molecular eigenvalues.[16] The ground-state configuration is thus

$$(A_1)^2(A_1)^2(B_2)^2(A_1)^2(B_1)^2\ .$$

The symmetry of the molecular orbitals is such that there are four orbitals of symmetry A_1 of the type

$$a\varphi_2(1s_O)+b\varphi_3(2s_O)+c\varphi_4(2p_{zO})$$
$$+d[\varphi_1(1s_{H1})+\varphi_7(1s_{H2})]\ ;\qquad(3.2)$$

one orbital of type B_1,

$$\varphi_6(2p_y)\ ;\qquad(3.3)$$

and two orbitals of type B_2,

$$f\varphi_5(2p_{xO})+g[\varphi_1(1s_{H1})-\varphi_7(1s_{H2})]\ .\qquad(3.4)$$

From the values of the coefficients of Table VI, we

TABLE V. Allowed optical transitions in the dipole approximation. We have indicated separately the case in which light is polarized parallel or perpendicular to the fourfold axis.

Initial states	Δ_1	Δ_1'	Δ_2	Δ_2'	Δ_5	Y_1	q_1	q_2
Final states with $\vec{e}$ parallel to the fourfold axis	Δ_1	Δ_1'	Δ_2	Δ_2'	Δ_5	Y_1	q_1	q_2
Final states with $\vec{e}$ perpendicular to the fourfold axis	Δ_5	Δ_5	Δ_5	Δ_5	$\Delta_1,\Delta_1',\Delta_2,\Delta_2'$	Y_1	q_1,q_2	q_1,q_2

TABLE VI. Minimal set expansion of the molecular orbitals of water in the intrinsic reference frame. Energies are in rydbergs and distance in Bohr radii (after Ref. 16).

| Center | $\vec{d}_1 = (1.431, 0, -1.109)$ | $\vec{d}_2 = 0$ | $\vec{d}_3 = 0$ | $\vec{d}_4 = 0$ | $\vec{d}_5 = 0$ | $\vec{d}_6 = 0$ | $\vec{d}_7 = (-1.431, 0, -1.109)$ |
| Expt. coefficient | 1.27 | 7.66 | 2.25 | 2.21 | 2.21 | 2.21 | 1.27 |
Slater-type functions	$\varphi_1(1s_{H1})$	$\varphi_2(1s_O)$	$\varphi_3(2s_O)$	$\varphi_4(2p_{zO})$	$\varphi_5(2p_{xO})$	$\varphi_6(2p_{yO})$	$\varphi_7(1s_{H2})$
$E_1 = -41.112$ A_1 ψ_1	-0.0036	0.9968	0.0152	-0.0032	0	0	-0.0036
$E_2 = -2.570$ A_1 ψ_2	0.1516	-0.2219	0.8426	-0.1320	0	0	0.1516
$E_3 = -1.249$ B_2 ψ_3	-0.4235	0	0	0	-0.6241	0	0.4235
$E_4 = -0.932$ A_1 ψ_4	-0.2646	-0.0934	0.5160	0.7870	0	0	-0.2646
$E_5 = -0.805$ B_1 ψ_5	0	0	0	0	0	1	0
$E_6 = -0.154$ A_1 ψ_6	0.8102	0.1218	-0.8841	0.7392	0	0	0.8102
$E_7 = -0.007$ B_2 ψ_7	0.8465	0	0	0	-0.9876	0	-0.8465

can also notice that the orbital ψ_1 is basically the $1s$ state of the oxygen atom; ψ_2 is a bonding combination of the $2s$ oxygen state both with $\varphi_4(2p_{zO})$ and with $\varphi_1(1s_{H1}) + \varphi_7(1s_{H2})$; ψ_3 is a bonding combination of $\varphi_5(2p_{xO})$ and $\varphi_1(1s_{H1}) - \varphi_7(1s_{H2})$; ψ_4 is a lone pair essentially formed with $\varphi_3(2s_O)$ and $\varphi_4(2p_{zO})$ states, the electron density being mainly in the z axis away from the hydrogens; ψ_5 is the $\varphi_6(2p_{yO})$ orbital and is another lone-pair orbital with electron density away from the plane of the molecule. The excited states ψ_6 and ψ_7 are antibonding orbitals with electron density mainly centered on the hydrogen atoms.

We wish to remark that the values of the energies E_6 and E_7 of Table VI have been obtained by including the exchange and Coulomb interaction of the excited orbital with the hole left in the molecule, since we will be interested in optical transitions.[18] The first molecular excitations in the Hartree-Fock approximation with the minimal set expansion are

$$E_6 - E_5 = 0.651 \text{ Ry} = 8.85 \text{ eV},$$

$$E_6 - E_4 = 0.778 \text{ Ry} = 10.58 \text{ eV}, \qquad (3.5)$$

$$E_7 - E_5 = 0.798 \text{ Ry} = 10.85 \text{ eV}.$$

Other calculations of the excited-state energies using a basis larger than the minimal one and different configurations are in agreement to within a few percent with (3.5).[17] From a physical point of view this agreement is not surprising because the first molecular excitations in water correspond to a transfer of an electron from a $2p$ oxygen state to a $1s$ hydrogen state, which are both included in the minimal set. For reasons of simplicity we will thus describe the ice electronic states starting from the minimal-set molecular orbitals of Table VI.

It is convenient to write explicitly the relationship between the internal frame of the two molecules per unit cell of Fig. 1 and the x, y, z axes

that constitute our basic reference frame. We have for molecule I

$$x_{int} = \tfrac{1}{2} \sqrt{2} (y + z),$$

$$y_{int} = \tfrac{1}{2} \sqrt{2} (y - z),$$

$$z_{int} = -x;$$

for molecule II

$$x_{int} = \tfrac{1}{2} \sqrt{2} (-y + z),$$

$$y_{int} = \tfrac{1}{2} \sqrt{2} (y + z), \qquad (3.6)$$

$$z_{int} = -x.$$

When the basic reference frame x, y, z is used, the coefficients of Table VI are to be changed in agreement with (3.6) and are reported in Table VII. Notice that the symmetry of the orbitals B_1 and B_2 of the second molecule are exchanged because the representations A_1, A_2, B_1, B_2 are referred to the first molecule in the unit cell.

B. Electronic States in Ice

As indicated in Fig. 1 we have two molecules per unit cell, and the basic molecular orbitals are

$$\psi_j^{(i)}(\vec{r}) = \sum_m a_{jm}^{(i)} \varphi_m(\vec{r} - \vec{d}_m^{(i)}), \qquad (3.7)$$

where $i = 1$, 2 labels the molecules, $j = 1, \ldots, 7$ labels the molecular orbitals in ascending order of energy, and φ_m are the appropriate Slater-type functions expressed in our basic x, y, z coordinate system as given in Table VII, where also the coefficients $a_{jm}^{(i)}$ and the positions $\vec{d}_m^{(i)}$ are reported. The number of molecular orbitals $\psi_j^{(i)}(\vec{r})$ is thus 14, because the minimal set has been adopted; the number of electrons per unit cell is 20. Starting from (3.7) we form the 14 molecular Bloch sums of vector $\vec{k}$:

$$\Phi_j^{(i)}(\vec{k}, \vec{r}) = \frac{1}{\sqrt{N}} \sum_{\vec{\tau}_\nu} e^{i\vec{k} \cdot \vec{\tau}_\nu} \psi_j^{(i)}(\vec{r} - \vec{\tau}_\nu)$$

$$= \frac{1}{\sqrt{N}} \sum_{\vec{\tau}_\nu} \sum_{m=1}^{7} e^{i\vec{k}\cdot\vec{\tau}_\nu} a_{jm}^{(i)} \, \varphi_m(\vec{r} - \vec{d}_m^{(i)} - \vec{\tau}_\nu) \, ,$$

$$(3.8)$$

where N is the number of unit cells in the crystal. At a general $\vec{k}$ vector the crystal energies are obtained as solutions of the determinantal equation

$$\|\langle \Phi_j^{(i)}(\vec{k}, \vec{r}) | H - E | \Phi_{j'}^{(i')}(\vec{k}, \vec{r})\rangle\| = 0 \, , \qquad (3.9)$$

where H is the crystal Hamiltonian. This is an extension of the standard tight-binding approach

obtained with the use of molecular orbitals instead of atomic orbitals. The use of the molecular Bloch sums automatically implies an important step toward self-consistency in treating atoms which belong to the same molecule.[19]

Let us now discuss the evaluation of the matrix elements of the determinant equation (3.9). We first consider the overlap matrix elements

$$S_{jj'}^{(ii')}(\vec{k}) = \langle \Phi_j^{(i)}(\vec{k}, \vec{r}) | \Phi_{j'}^{(i')}(\vec{k}, \vec{r})\rangle \, ,$$

which, because of Eq. (3.8) yields

$$S_{jj'}^{(ii')}(\vec{k}) = \left\langle \frac{1}{\sqrt{N}} \sum_{\vec{\tau}_\nu} \sum_{m=1}^{7} e^{i\vec{k}\cdot\vec{\tau}_\nu} a_{jm}^{(i)} \varphi_m(\vec{r} - \vec{d}_m^{(i)} - \vec{\tau}_\nu) \left| \frac{1}{\sqrt{N}} \sum_{\vec{\tau}_\nu} \sum_{m'=1}^{7} e^{i\vec{k}\cdot\vec{\tau}_\nu} a_{j'm'}^{(i')} \varphi_{m'}(\vec{r} - \vec{d}_{m'}^{(i')} - \vec{\tau}_\nu') \right. \right\rangle$$

$$= \sum_{\vec{\tau}_\nu} \sum_{m,m'=1}^{7} e^{i\vec{k}\cdot\vec{\tau}'} a_{jm}^{(i)} a_{j'm'}^{(i')} \langle \varphi_m(\vec{r} - \vec{d}_m^{(i)}) | \varphi_{m'}(\vec{r} - \vec{d}_{m'}^{(i')} - \vec{\tau}_\nu')\rangle \, , \qquad (3.10)$$

where the $\sum_{\vec{\tau}_\nu}$ has just cancelled the denominator $1/N$. The matrix elements of the type $\langle \varphi_m(\vec{r} - \vec{d}_m^{(i)}) | \varphi_{m'}(\vec{r} - \vec{d}_{m'}^{(i')} - \vec{\tau}_\nu')\rangle$ decrease rapidly with increasing the two-center distance $|\vec{d}_{m'}^{(i')} + \vec{\tau}_\nu'$

$- \vec{d}_m^{(i)}|$; for our purpose it was sufficient to include first-, second-, third-, and fourth-neighbor interactions. Following the procedure of Slater and Koster,[20] the matrix elements $\langle \varphi_m(\vec{r} - \vec{d}_m^{(i)})$

TABLE VII. Minimal set expansion of the molecular orbitals of the two water molecules per unit cell in the basic reference frame of Fig. 1.

Center	$\vec{d}_1^{(1)}$	$\vec{d}_2^{(1)}$	$\vec{d}_3^{(1)}$	$\vec{d}_4^{(1)}$	$\vec{d}_5^{(1)}$	$\vec{d}_6^{(1)}$	$\vec{d}_7^{(1)}$
Expt. coefficient	1.27	7.66	2.25	2.21	2.21	2.21	1.27
Slater functions	$\varphi_1(1s_{H1})$	$\varphi_2(1s_O)$	$\varphi_3(2s_O)$	$\varphi_4(2p_{x.O})$	$\varphi_5(2p_{yO})$	$\varphi_6(2p_{zO})$	$\varphi_7(1s_{H2})$
$E_1^{(1)}=E_1 \quad A_1 \quad \psi_1^{(1)}$	a_{11}	a_{12}	a_{13}	$-a_{14}$	0	0	a_{17}
$E_2^{(1)}=E_2 \quad A_1 \quad \psi_2^{(1)}$	a_{21}	a_{22}	a_{23}	$-a_{24}$	0	0	a_{27}
$E_3^{(1)}=E_3 \quad B_2 \quad \psi_3^{(1)}$	a_{31}	0	0	0	$\frac{1}{2}\sqrt{2}\,a_{35}$	$\frac{1}{2}\sqrt{2}\,a_{35}$	a_{37}
$E_4^{(1)}=E_4 \quad A_1 \quad \psi_4^{(1)}$	a_{41}	a_{42}	a_{43}	$-a_{44}$	0	0	a_{47}
$E_5^{(1)}=E_5 \quad B_1 \quad \psi_5^{(1)}$	0	0	0	0	$\frac{1}{2}\sqrt{2}$	$-\frac{1}{2}\sqrt{2}$	0
$E_6^{(1)}=E_6 \quad A_1 \quad \psi_6^{(1)}$	a_{61}	a_{62}	a_{63}	$-a_{64}$	0	0	a_{67}
$E_7^{(1)}=E_7 \quad B_2 \quad \psi_7^{(1)}$	a_{71}	0	0	0	$\frac{1}{2}\sqrt{2}\,a_{75}$	$\frac{1}{2}\sqrt{2}\,a_{75}$	a_{77}

$$\vec{d}^{(1)} = \tfrac{1}{8}a_0(\beta,\beta,\beta); \quad \vec{d}_2^{(1)}=\vec{d}_3^{(1)}=\vec{d}_4^{(1)}=\vec{d}_5^{(1)}=\vec{d}_6^{(1)}=0; \quad \vec{d}_7^{(1)}=\tfrac{1}{8}a_0(\beta,-\beta,-\beta)$$

Center	$\vec{d}_1^{(2)}$	$\vec{d}_2^{(2)}$	$\vec{d}_3^{(2)}$	$\vec{d}_4^{(2)}$	$\vec{d}_5^{(2)}$	$\vec{d}_6^{(2)}$	$\vec{d}_7^{(2)}$
Expt. coefficient	1.27	7.66	2.25	2.21	2.21	2.21	1.27
Slater functions	$\varphi_1(1s_{H1})$	$\varphi_2(1s_O)$	$\varphi_3(2s_O)$	$\varphi_4(2s_{xO})$	$\varphi_5(2p_{yO})$	$\varphi_6(2p_{zO})$	$\varphi_7(1s_{H2})$
$E_1^{(2)}=E_1 \quad A_1 \quad \psi_1^{(2)}$	a_{11}	a_{12}	a_{13}	$-a_{14}$	0	0	a_{17}
$E_2^{(2)}=E_2 \quad A_1 \quad \psi_2^{(2)}$	a_{21}	a_{22}	a_{23}	$-a_{24}$	0	0	a_{27}
$E_3^{(2)}=E_3 \quad B_1 \quad \psi_3^{(2)}$	a_{31}	0	0	0	$-\frac{1}{2}\sqrt{2}\,a_{35}$	$\frac{1}{2}\sqrt{2}\,a_{35}$	a_{37}
$E_4^{(2)}=E_4 \quad A_1 \quad \psi_4^{(2)}$	a_{41}	a_{42}	a_{43}	$-a_{44}$	0	0	a_{47}
$E_5^{(2)}=E_5 \quad B_2 \quad \psi_5^{(2)}$	0	0	0	0	$\frac{1}{2}\sqrt{2}$	$\frac{1}{2}\sqrt{2}$	0
$E_6^{(2)}=E_6 \quad A_1 \quad \psi_6^{(2)}$	a_{61}	a_{62}	a_{63}	$-a_{64}$	0	0	a_{67}
$E_7^{(2)}=E_7 \quad B_1 \quad \psi_7^{(2)}$	a_{71}	0	0	0	$-\frac{1}{2}\sqrt{2}\,a_{75}$	$\frac{1}{2}\sqrt{2}\,a_{75}$	a_{77}

$$\vec{d}_1^{(2)} = \tfrac{1}{8}a_0(\beta+2,-\beta+2,\beta+2); \quad \vec{d}_2^{(2)}=\vec{d}_3^{(2)}=\vec{d}_4^{(2)}=\vec{d}_5^{(2)}=\vec{d}_6^{(2)}=\tfrac{1}{4}a_0(1,1,1); \quad \vec{d}_7^{(2)}=\tfrac{1}{8}a_0(\beta+2,\beta+2,-\beta+2)$$

TABLE VIII. Values of the overlap and the kinetic-energy integrals. The notations used are taken from Ref. 20. The two-center distances are discussed in Sec. II.

Two-center distance	Overlap integrals	Kinetic-energy integrals (in Ry)
5.52	$S_1(1s_H\ 1s_H\sigma) = 0.0221$	$P_1(1s_H\ 1s_H\sigma) = -0.0122$
4.34	$S_2(1s_H\ 1s_H\sigma) = 0.0674$	$P_2(1s_H\ 1s_H\sigma) = -0.0236$
3.36	$S_3(1s_H\ 2s_O\sigma) = 0.1167$	$P_3(1s_H\ 2s_O\sigma) = -0.0368$
5.20	$S_4(2s_O\ 2s_O\sigma) = 0.0055$	$P_4(2s_O\ 2s_O\sigma) = -0.0098$
3.36	$S_5(1s_H\ 2p_O\sigma) = -0.1267$	$P_5(1s_H\ 2p_O\sigma) = -0.0031$
5.20	$S_6(2s_O\ 2p_O\sigma) = -0.0088$	$P_6(2s_O\ 2p_O\sigma) = 0.0135$
5.20	$S_7(2p_O\ 2p_O\sigma) = -0.0135$	$P_7(2p_O\ 2p_O\sigma) = 0.0169$
5.20	$S_8(2p_O\ 2p_O\pi) = 0.0017$	$P_8(2p_O\ 2p_O\pi) = -0.0027$
3.36	$S_9(1s_H\ 1s_O\sigma) = 0.0078$	$P_9(1s_H\ 1s_O\sigma) = -0.0065$
5.20	$S_{10}(1s_O\ 2p_O\sigma) = -0.0002$	$P_{10}(1s_O\ 2p_O\sigma) = 0.0005$
5.20	$S_{11}(1s_O\ 2s_O\sigma) = 0.0001$	$P_{11}(1s_O\ 2s_O\sigma) = -0.0003$

$\times\ |\varphi_{m'}(\vec{r} - \vec{d}_{m'}^{(i')} - \vec{\tau}_\nu')\rangle$ for all neighbors of a given order have been expressed in terms of independent integrals, which are reported in Table VIII. Thus, using Table VIII for the independent integrals, applying the procedure of Slater and Koster, and using Table VII for the coefficients $a_{jm}^{(i)}$ and $a_{jm'}^{(i')}$, the overlap matrix elements $S_{jj'}^{(ii')}(\vec{k})$ can be explicitly obtained.

A similar procedure has been applied to the calculation of the kinetic-operator matrix elements:

$$P_{jj'}^{(ii')}(\vec{k}) = \langle \Phi_j^{(i)}(\vec{k}, \vec{r})\ |\ p^2/2m\ |\ \Phi_{j'}^{(i')}(\vec{k}, \vec{r})\rangle$$

$$= \sum_{\vec{\tau}_\nu} \sum_{m,m'=1}^{7} e^{i\vec{k}\cdot\vec{\tau}_\nu} a_{jm}^{(i)} a_{j'm'}^{(i')} \langle \varphi_m(\vec{r} - \vec{d}_m^{(i)})$$

$$\times\ |\ p^2/2m\ |\ \varphi_{m'}(\vec{r} - \vec{d}_{m'}^{(i')} - \vec{\tau}_\nu')\rangle\ . \quad (3.11)$$

The independent kinetic-energy integrals are also reported in Table VIII.

The Hamiltonian matrix elements

$$H_{jj'}^{(ii')}(\vec{k}) = \langle \Phi_j^{(i)}(\vec{k}, \vec{r})\ |\ H\ |\ \Phi_{j'}^{(i')}(\vec{k}, \vec{r})\rangle \quad (3.12)$$

can easily be expressed in terms of $S_{jj'}^{(ii')}(\vec{k})$ and $P_{jj'}^{(ii')}(\vec{k})$ if one neglects three-center integrals and crystal field integrals. In Appendix A we justify these approximations for our case, and we derive the following expression for (3.12):

$$H_{jj'}^{(ii')}(\vec{k}) = (E_j + E_{j'})S_{jj'}^{(ii')}(\vec{k}) - P_{jj'}^{(ii')}(\vec{k})$$

$$- \delta_{ii'}[E_j\delta_{jj'} - \langle \psi_j^{(i)}(\vec{r})\ |\ p^2/2m\ |\ \psi_{j'}^{(i')}(\vec{r})\rangle]\ . \quad (3.13)$$

Using Eqs. (3.10), (3.11), and (3.13), the matrix elements of the determinant equation (3.9) can explicitly be set up.

At high-symmetry points or lines the order of the determinant equation (3.9) can be reduced by considering the symmetrized combinations of molecular Bloch sums reported in Table IX.

In Table X we give the matrix elements of the determinant equation (3.9) at the symmetry points Δ, X, Y, L and at the symmetry lines p, q, l. From physical considerations (see energy sequence) and from numerical precision considerations (see Sec. IV) we assume that the Bloch sums $\Phi_1^{(1)}$, $\Phi_1^{(2)}$ interact only among themselves, giving two very

TABLE IX. Symmetrized combinations of molecular Bloch sums at the symmetry points Δ, X, Y, L and at the symmetry lines p, q, l. For the two-dimensional representations partner functions are indicated with brackets. The phase factor $e^{i\pi p/2}$ equals 1 at the point Δ and equals $+i$ at the point X.

Irreducible representation	Symmetrized combinations of molecular Bloch sums
Δ_1 or p_1 or X_1	$\frac{1}{2}\sqrt{2}[\Phi_1^{(1)} + e^{i\pi p/2}\Phi_1^{(2)}]$; $\frac{1}{2}\sqrt{2}[\Phi_2^{(1)} + e^{i\pi p/2}\Phi_2^{(2)}]$; $\frac{1}{2}\sqrt{2}[\Phi_4^{(1)} + e^{i\pi p/2}\Phi_4^{(2)}]$; $\frac{1}{2}\sqrt{2}[\Phi_6^{(1)} + e^{i\pi p/2}\Phi_6^{(2)}]$
Δ_2' or p_2' or X_2'	The symmetrized combinations are obtained from those of Δ_1 or p_1 or X_1 by replacing the phase factor $e^{i\pi p/2}$ with $-e^{i\pi p/2}$.
Δ_5 or p_5 or X_5	$\begin{cases}\Phi_3^{(1)}\\-\Phi_3^{(2)}\end{cases}$; $\begin{cases}\Phi_5^{(2)}\\\Phi_5^{(1)}\end{cases}$; $\begin{cases}\Phi_7^{(1)}\\-\Phi_7^{(2)}\end{cases}$
q_1	$\frac{1}{2}\sqrt{2}[\Phi_1^{(1)} + e^{i\pi q/2}\Phi_1^{(2)}]$; $\frac{1}{2}\sqrt{2}[\Phi_2^{(1)} + e^{i\pi q/2}\Phi_2^{(2)}]$, $\frac{1}{2}\sqrt{2}[\Phi_3^{(1)} - e^{i\pi q/2}\Phi_3^{(2)}]$, $\frac{1}{2}\sqrt{2}[\Phi_4^{(1)} + e^{i\pi q/2}\Phi_4^{(2)}]$; $\frac{1}{2}\sqrt{2}[\Phi_5^{(1)} + e^{i\pi q/2}\Phi_5^{(2)}]$; $\frac{1}{2}\sqrt{2}[\Phi_6^{(1)} + e^{i\pi q/2}\Phi_6^{(2)}]$; $\frac{1}{2}\sqrt{2}[\Phi_7^{(1)} - e^{i\pi q/2}\Phi_7^{(2)}]$.
q_2	The symmetrized combinations are obtained from those of q_1 by replacing the phase factor $e^{i\pi q/2}$ with $-e^{i\pi q/2}$.
Y_1	$\begin{cases}\Phi_1^{(1)}\\\Phi_1^{(2)}\end{cases}$; $\begin{cases}\Phi_2^{(1)}\\\Phi_2^{(2)}\end{cases}$; $\begin{cases}\Phi_3^{(1)}\\-\Phi_3^{(2)}\end{cases}$; $\begin{cases}\Phi_4^{(1)}\\\Phi_4^{(2)}\end{cases}$; $\begin{cases}\Phi_5^{(1)}\\\Phi_5^{(2)}\end{cases}$; $\begin{cases}\Phi_6^{(1)}\\\Phi_6^{(2)}\end{cases}$; $\begin{cases}\Phi_7^{(1)}\\-\Phi_7^{(2)}\end{cases}$
l_1 or L_1	$\Phi_1^{(1)}$; $\Phi_1^{(2)}$; $\Phi_2^{(1)}$; $\Phi_2^{(2)}$; $\Phi_3^{(1)}$; $\Phi_4^{(1)}$; $\Phi_4^{(2)}$; $\Phi_5^{(2)}$; $\Phi_6^{(1)}$; $\Phi_6^{(2)}$; $\Phi_7^{(1)}$
l_2 or L_2	$-\Phi_3^{(2)}$; $\Phi_5^{(1)}$; $-\Phi_7^{(2)}$

TABLE X. Matrix elements of the crystal Hamiltonian among the symmetrized combinations of Table IX.

Matrix order	Matrix elements
1×1	p_1 (one core state) $M_{11} = (2E_1 - E)[1 + O(2)_{11} + O(1)_{11}\cos\frac{1}{2}\pi p] - K(2)_{11} - K(1)_{11}\cos\frac{1}{2}\pi p - E_1$
1×1	p_1 (one deep valence state) $M_{11} = (2E_2 - E)[1 + O(2)_{22} + O(1)_{22}\cos\frac{1}{2}\pi p] - K(2)_{22} - K(1)_{22}\cos\frac{1}{2}\pi p - E_2$
2×2	p_1 (one valence state and one excited state) $M_{11} = (2E_4 - E)[1 + O(2)_{44} + O(1)_{44}\cos\frac{1}{2}\pi p] - K(2)_{44} - K(1)_{44}\cos\frac{1}{2}\pi p - E_4$ $M_{22} = (2E_6 - E)[1 + O(2)_{66} + O(1)_{66}\cos\frac{1}{2}\pi p] - K(2)_{66} - K(1)_{66}\cos\frac{1}{2}\pi p - E_6$ $M_{12} = M_{21}^* = (E_4 + E_6 - E)[O(2)_{46} + O(1)_{46}\cos\frac{1}{2}\pi p] - K(2)_{46} - K(1)_{46}\cos\frac{1}{2}\pi p$

The matrix elements of the representation p_2' are obtained from the matrix elements of the representation p_1 by replacing
$$\cos\tfrac{1}{2}\pi p \text{ with } - \cos\tfrac{1}{2}\pi p.$$

3×3	p_5 (two doubly degenerate valence states and one doubly degenerate excited state) $M_{11} = (2E_3 - E)[1 - O(2)_{33}] + K(2)_{33} - E_3; \quad M_{22} = E_5 - E$ $M_{33} = (2E_7 - E)[1 - O(2)_{77}] + K(2)_{77} - E_7$ $M_{12} = M_{21}^* = (E_3 + E_5 - E)[O(3)_3 + O(4)_3 e^{-i\pi p}] - K(3)_3 - K(4)_3 e^{-i\pi p}$ $M_{13} = M_{31}^* = (E_3 + E_7 - E)[- O(2)_{37}] + K(2)_{37}$ $M_{23} = M_{32}^* = (E_5 + E_7 - E)[O(3)_7 + O(4)_7 e^{i\pi p}] - K(3)_7 - K(4)_7 e^{i\pi p}$

The matrix elements of the representations Δ_1, Δ_2', Δ_5 and X_1, X_2', X_5 are obtained from the matrix elements of the representations p_1, p_2', p_5 by replacing p with 0 and 1, respectively.

1×1	q_1 (one core state) $M_{11} = (2E_1 - E)[1 + O(2)_{11}\cos\pi q + O(1)_{11}\cos\frac{1}{2}\pi q] - K(2)_{11}\cos\pi q - K(1)_{11}\cos\frac{1}{2}\pi q - E_1$
1×1	q_1 (one deep valence state) $M_{11} = (2E_2 - E)[1 + O(2)_{22}\cos\pi q + O(1)_{22}\cos\frac{1}{2}\pi q] - K(2)_{22}\cos\pi q - K(1)_{22}\cos\frac{1}{2}\pi q - E_2$
5×5	q_1 (three valence states and two excited states) $M_{11} = (2E_3 - E)[1 - O(2)_{33}\cos\pi q] + K(2)_{33} - E_3$ $M_{22} = (2E_4 - E)[1 + O(2)_{44}\cos\pi q + O(1)_{44}\cos\frac{1}{2}\pi q] - K(2)_{44}\cos\pi q - K(1)_{44}\cos\frac{1}{2}\pi q - E_4$ $M_{33} = E_5 - E; \quad M_{44} = (2E_6 - E)[1 + O(2)_{66}\cos\pi q + O(1)_{66}\cos\frac{1}{2}\pi q] - K(2)_{66}\cos\pi q - K(1)_{66}\cos\frac{1}{2}\pi q - E_6$ $M_{55} = (2E_7 - E)[1 - O(2)_{77}\cos\pi q] + K(2)_{77}\cos\pi q - E_7$ $M_{12} = M_{21}^* = (E_3 + E_4 - E)[O(5)_{43}i\sin\pi q - O(6)_{43}i\sin\frac{1}{2}\pi q] - K(5)_{43}i\sin\pi q + K(6)_{43}i\sin\frac{1}{2}\pi q$ $M_{13} = M_{31}^* = (E_3 + E_5 - E)[O(3)_3 + O(4)_3]\cos\frac{1}{2}\pi q - [K(3)_3 + K(4)_3]\cos\frac{1}{2}\pi q$ $M_{14} = M_{41}^* = (E_3 + E_6 - E)[O(5)_{63}i\sin\pi q + O(6)_{63}i\sin\frac{1}{2}\pi q] - K(5)_{63}i\sin\pi q - K(6)_{63}i\sin\frac{1}{2}\pi q$ $M_{15} = M_{51}^* = (E_3 + E_7 - E)[- O(2)_{37}\cos\pi q] + K(2)_{37}\cos\pi q$ $M_{23} = M_{32}^* = (E_4 + E_5 - E)[O(7)_4 i\sin\frac{1}{2}\pi q] - K(7)_4 i\sin\frac{1}{2}\pi q$ $M_{24} = M_{42}^* = (E_4 + E_6 - E)[O(2)_{46}\cos\pi q + O(1)_{46}\cos\frac{1}{2}\pi q] - K(2)_{46}\cos\pi q - K(1)_{46}\cos\frac{1}{2}\pi q$ $M_{25} = M_{52}^* = (E_4 + E_7 - E)[- O(5)_{47}i\sin\pi q - O(6)_{47}i\sin\frac{1}{2}\pi q] + K(5)_{47}i\sin\pi q + K(6)_{47}i\sin\frac{1}{2}\pi q$ $M_{34} = M_{43}^* = (E_5 + E_6 - E)[- O(7)_6 i\sin\frac{1}{2}\pi q] + K(7)_6 i\sin\frac{1}{2}\pi q$. $M_{35} = M_{53}^* = (E_5 + E_7 - E)[O(3)_7 + O(4)_7]\cos\frac{1}{2}\pi q - [K(3)_7 + K(4)_7]\cos\frac{1}{2}\pi q$ $M_{45} = M_{54}^* = (E_6 + E_7 - E)[- O(5)_{67}i\sin\pi q - O(6)_{67}i\sin\frac{1}{2}\pi q] + K(5)_{67}i\sin\pi q + K(6)_{67}i\sin\frac{1}{2}\pi q$

Note: For $q = 0$ the above 5×5 determinant is split in a determinant 3×3 (Δ_5 states) and a determinant 2×2 (Δ_1 states).

The matrix elements of the representation q_2 are obtained from the matrix elements of the representation q_1 by replacing $\sin\frac{1}{2}\pi q$ and $\cos\frac{1}{2}\pi q$ with $- \sin\frac{1}{2}\pi q$ and $- \cos\frac{1}{2}\pi q$, respectively.

The matrix elements of the representation Y_1 are obtained either from the matrix elements of q_1 or from those of q_2 by putting $q = 1$.

TABLE X. (Continued).

Matrix order	Matrix elements

l_1 (two core states)

$$M_{11} = (2E_1 - E)[1 + O(2)_{11}\cos\pi l] - K(2)_{11}\cos\pi l - E_1$$

2 × 2

$$M_{22} = (2E_1 - E)[1 + O(2)_{11}] - K(2)_{11} - E_1$$

$$M_{12} = M_{21}^* = (2E_1 - E)[O(1)_{11}\tfrac{1}{4}(1 + 3e^{-i\pi l})] - K(1)_{11}\tfrac{1}{4}(1 + 3e^{-i\pi l})$$

The matrix elements of the representation l_1 for the two deep valence states are obtained from those of the representation l_1 for the two core states by replacing E_1, $O(1)_{11}$, $O(2)_{11}$, $K(1)_{11}$, $K(2)_{11}$ with E_2, $O(1)_{22}$, $O(2)_{22}$, $K(1)_{22}$, $K(2)_{22}$, respectively.

l_1 (four valence states and three excited states)

$$M_{11} = (2E_3 - E)[1 - O(2)_{33}\cos\pi l] + K(2)_{33}\cos\pi l - E_3$$

$$M_{22} = (2E_4 - E)[1 + O(2)_{44}\cos\pi l] - K(2)_{44}\cos\pi l - E_4$$

$$M_{33} = (2E_4 - E)[1 + O(2)_{44}] - K(2)_{44} - E_4; \quad M_{44} = E_5 - E$$

$$M_{55} = (2E_6 - E)[1 + O(2)_{66}\cos\pi l] - K(2)_{66}\cos\pi l - E_6$$

$$M_{66} = (2E_6 - E)[1 + O(2)_{66}] - K(2)_{66} - E_6$$

$$M_{77} = (2E_7 - E)[1 - O(2)_{77}\cos\pi l] + K(2)_{77}\cos\pi l - E_7$$

$$M_{12} = M_{21}^* = (E_3 + E_4 - E)O(5)_{43}\tfrac{1}{2}i\,\sin\pi l - K(5)_{43}\tfrac{1}{2}i\,\sin\pi l$$

$$M_{13} = M_{31}^* = (E_3 + E_4 - E)O(6)_{43}\tfrac{1}{2}(1 - e^{-i\pi l}) - K(6)_{43}\tfrac{1}{2}(1 - e^{-i\pi l})$$

$$M_{14} = M_{41}^* = (E_3 + E_5 - E)[O(3)_3 e^{-i\pi l} + O(4)_3\tfrac{1}{2}(1 + e^{-i\pi l})] - [K(3)_3 e^{-i\pi l} + K(4)_3\tfrac{1}{2}(1 + e^{-i\pi l})]$$

7 × 7

$$M_{15} = M_{51}^* = (E_3 + E_6 - E)O(5)_{63}\tfrac{1}{2}i\,\sin\pi l - K(5)_{63}\tfrac{1}{2}i\,\sin\pi l$$

$$M_{16} = M_{61}^* = (E_3 + E_6 - E)O(6)_{63}\tfrac{1}{2}(1 - e^{-i\pi l}) - K(6)_{63}\tfrac{1}{2}(1 - e^{-i\pi l})$$

$$M_{17} = M_{71}^* = (E_3 + E_7 - E)[- O(2)_{37}\cos\pi l] + K(2)_{37}\cos\pi l$$

$$M_{23} = M_{32}^* = (2E_4 - E)[O(1)_{44}\tfrac{1}{4}(1 + 3e^{-i\pi l})] - K(1)_{44}\tfrac{1}{4}(1 + 3e^{-i\pi l})$$

$$M_{24} = M_{42}^* = (E_4 + E_5 - E)[O(7)_4\tfrac{1}{2}(-1 + e^{-i\pi l})] - K(7)_4\tfrac{1}{2}(-1 + e^{-i\pi l})$$

$$M_{25} = M_{52}^* = (E_4 + E_6 - E)[O(2)_{46}\cos\pi l] - K(2)_{46}\cos\pi l$$

$$M_{26} = M_{62}^* = (E_4 + E_6 - E)[O(1)_{46}\tfrac{1}{4}(1 + 3e^{-i\pi l})] - K(1)_{46}\tfrac{1}{4}(1 + 3e^{-i\pi l})$$

$$M_{27} = M_{72}^* = (E_4 + E_7 - E)[- O(5)_{47}\tfrac{1}{2}i\,\sin\pi l] + K(5)_{47}\tfrac{1}{2}i\,\sin\pi l; \quad M_{34} = M_{43} = 0$$

$$M_{35} = M_{53}^* = (E_4 + E_6 - E)[O(1)_{46}\tfrac{1}{4}(1 + 3e^{i\pi l})] - K(1)_{46}\tfrac{1}{4}(1 + 3e^{i\pi l}); \quad M_{36} = M_{63}^* = M_{25}$$

$$M_{37} = M_{73}^* = (E_4 + E_7 - E)[O(6)_{47}\tfrac{1}{2}(1 - e^{i\pi l})] - K(6)_{47}\tfrac{1}{2}(1 - e^{i\pi l})$$

$$M_{45} = M_{54}^* = (E_5 + E_6 - E)[O(7)_6\tfrac{1}{2}(-1 + e^{i\pi l})] - K(7)_6\tfrac{1}{2}(-1 + e^{i\pi l}); \quad M_{46} = M_{64} = 0$$

$$M_{47} = M_{74}^* = (E_5 + E_7 - E)[O(3)_7 e^{i\pi l} + O(4)_7\tfrac{1}{2}(1 + e^{i\pi l})] - [K(3)_7 e^{i\pi l} + K(4)_7\tfrac{1}{2}(1 + e^{i\pi l})]$$

$$M_{56} = M_{65}^* = (2E_6 - E)[O(1)_{66}\tfrac{1}{4}(1 + 3e^{-i\pi l})] - K(1)_{66}\tfrac{1}{4}(1 + 3e^{-i\pi l})$$

$$M_{57} = M_{75}^* = (E_6 + E_7 - E)[- O(5)_{67}\tfrac{1}{2}i\,\sin\pi l] + K(5)_{67}\tfrac{1}{2}i\,\sin\pi l$$

$$M_{67} = M_{76}^* = (E_6 + E_7 - E)[O(6)_{67}\tfrac{1}{2}(1 - e^{i\pi l})] - K(6)_{67}\tfrac{1}{2}(1 - e^{i\pi l})$$

Note: for $l = 0$ the above 7 × 7 determinant is factorized in a determinant 3 × 3 (Δ_5 states) and two determinants 2 × 2 (Δ_1 states and Δ_2' states).

l_2 (two valence states and one excited state)

$$M_{11} = (2E_3 - E)[1 - O(2)_{33}] + K(2)_{33} - E_3; \quad M_{22} = E_5 - E$$

$$M_{33} = (2E_7 - E)[1 - O(2)_{77}] + K(2)_{77} - E_7$$

3 × 3

$$M_{12} = M_{21}^* = (E_5 + E_5 - E)[O(8)_3 + O(9)_3 e^{i\pi l}] - [K(8)_3 + K(9)_3 e^{i\pi l}]$$

$$M_{13} = M_{31}^* = (E_3 + E_7 - E)[- O(2)_{37}] + K(2)_{37}$$

$$M_{23} = M_{32}^* = (E_5 + E_7 - E)[O(8)_7 + O(9)_7 e^{-i\pi l}] - [K(8)_7 + K(9)_7 e^{-i\pi l}]$$

The matrix elements of the representations L_1, L_2, are obtained from the matrix elements of the representations l_1, l_2 by putting $l = 1$.

TABLE X. (Continued).

Matrix order	Matrix elements

<div align="center">Meaning of the symbols used</div>

$$O(1)_{ij} = 8 a_{i1} a_{j1} S_2 + 2(a_{i1} a_{j3} + a_{j1} a_{i3}) S_3 + 4 a_{i3} a_{j3} S_4 + \tfrac{2}{3}\sqrt{3}\,(a_{i1} a_{j4} + a_{j1} a_{i4}) S_5$$
$$+ \tfrac{4}{3} a_{i4} a_{j4} S_7 + \tfrac{8}{3} a_{i4} a_{j4} S_8$$

$$O(2)_{ij} = 2 a_{i1} a_{j1} S_1$$

$$O(3)_i = 2 a_{i5} S_7; \quad O(4)_i = \tfrac{2}{3}\sqrt{6}\, a_{i1} S_5 + \tfrac{4}{3} a_{i5} S_7 + \tfrac{2}{3} a_{i5} S_8$$

$$O(5)_{ij} = 4 a_{i1} a_{j3} S_1$$

$$O(6)_{ij} = 4 a_{i1} a_{j3} S_2 + 2 a_{i3} a_{j1} S_3 - \tfrac{2}{3}\sqrt{3}\, a_{i4} a_{j1} S_5 - \tfrac{2}{3}\sqrt{6}\, a_{i3} a_{j5} S_6 - \tfrac{2}{3}\sqrt{6}\, a_{i4} a_{j5}(S_7 - S_8)$$

$$O(7)_i = -\tfrac{2}{3}\sqrt{6}\, a_{i1} S_5 - \tfrac{2}{3}\sqrt{6}\, a_{i3} S_6 + \tfrac{2}{3}\sqrt{6}\, a_{i4}(S_7 - S_8)$$

$$O(8)_i = \tfrac{1}{3}\sqrt{6}\, a_{i1} S_5 + a_{i5} S_8$$

$$O(9)_i = \tfrac{1}{3}\sqrt{6}\, a_{i1} S_5 + \tfrac{4}{3} a_{i5} S_7 + \tfrac{5}{3} a_{i5} S_8$$

$K(1)_{ij}, K(2)_{ij}, \ldots K(9)_i$ are obtained from $O(1)_{ij}, O(2)_{ij}, \ldots O(9)_i$ by replacing the overlap integrals S with the kinetic energy integrals P.

low core states. We also assume that the Bloch sums $\Phi_2^{(1)}$, $\Phi_2^{(2)}$ interact only among themselves giving two deep valence states. The remaining ten Bloch sums $\Phi_3^{(1)}$, $\Phi_3^{(2)}$, $\Phi_4^{(1)}$, $\Phi_4^{(2)}$, $\Phi_5^{(1)}$, $\Phi_5^{(2)}$, $\Phi_6^{(1)}$, $\Phi_6^{(2)}$, $\Phi_7^{(1)}$, $\Phi_7^{(2)}$ give six valence states and four excited states.[18] Despite its length, Table X is explicitly reported because it is very useful to reobtain cubic-ice band structure in the case of an improvement of the theoretical calculation of the excited molecular orbitals and energies of water. Table X is also very useful for pseudopotentials[21] or interpolation applications[20] to obtain, for instance, effective masses, density of states, oscillator strengths, and dependence of the electronic states on pressure.

IV. BAND STRUCTURE AND OPTICAL PROPERTIES

Starting from the self-consistent water-molecule calculations of Table VI, and using Tables VIII and X, the band structure of CIMS has been calculated from the determinant equation (3.9). No semiempirical adjustment to experimental data has been made. The crystal energies have been calculated beside the symmetry points Δ, X, Y, L in 50 points along each of the symmetry lines p, q, l. The relevant crystal energies are reported in Table XI and the band structure is shown in Figs. 4 and 5.

We wish first to comment on the numerical precision of our results in CIMS. At every $\vec{k}$ vector, we have neglected the interaction of the two core states and the two deep valence states with the other valence and excited states. This assumption has been tested and justified at some selected points of the Brillouin zone. The valence bands have been computed both including and neglecting

their interactions with excited bands and are found to be insensitive within less than 1% to a similar change. The reliability of the excited bands could be checked only by adding new orbitals to the minimal set; however, the small effect that this has in the free molecule gives confidence that also excited bands are meaningful.

We wish now to comment on the meaningfulness of the adopted model. In CIMS the direction x and the directions y, z are not equivalent because of the fourfold axis of the group C_{4v}. However, from Figs. 4(b) and 5 we notice that the energy of an electron with a given $\vec{k}$ vector is almost the same when $\vec{k}$ is along the x direction (line p) or the y, z directions (line q), the maximum difference being 0.001, 0.06, 0.15, and 0.29 eV for core bands, deep valence bands, valence bands, and excited bands, respectively. Thus, the energy bands of CIMS are almost cubiclike. This fact is expected in the case of a spherically symmetric distribution of the electronic cloud in water molecules and constitutes an a posteriori proof of the validity of such an assumption. More generally, using the Slater and Koster procedure,[20] we have tested this assumption by comparing the expressions of the overlap integrals, the kinetic-energy integrals, and the Hamiltonian integrals between two nearest-neighbor molecules in the three different relative orientations.[22] In these expressions, we have noticed that the dominant contributions were independent of the orientation; the small differences, treated in a perturbation way, are estimated to produce, at most, variation of the order of 0.1 eV in the energy-band levels. The basic physical assumption of CIMS is thus justified.

From Fig. 4, we see that the fundamental edge

occurs at $\vec{k} = 0$ between the Δ_5 valence state and the Δ_2' excited state, with an energy gap of 7.8 eV. The sequence of crystal states at $\vec{k} = 0$ is in substantial agreement with the previous results obtained by us in a semiempirical way.[10]

It is interesting to compare the sequence of molecular states with the sequence of crystal states at $\vec{k} = 0$ (Fig. 4). We notice that the degenerate orbitals of symmetry B_1 (or B_2) of the first molecule and B_2 (or B_1) of the second molecule are still degenerate and become the crystal state Δ_5. Instead the orbitals of symmetry A_1 interact to produce a considerable Davydov splitting[23] into the crystal states Δ_1 and Δ_2'. From Table XI we see that the splitting $E(\Delta_2') - E(\Delta_1)$ equals -0.14 eV for the core states, 5.14 eV for the deep valence states, 1.03 eV for the valence states, and -1.92 eV for the excited states. The sign of the above Davydov splittings and the reason for the relative wide energy separation between the deep valence

states Δ_1 and Δ_2' can be understood from Table IX, by observing that the combination $\frac{1}{2}\sqrt{2}[\Phi_2^{(1)} + \Phi_2^{(2)}]$ (deep valence state Δ_1) increases the electron density between the two molecules per unit cell in a more effective way than $\frac{1}{2}\sqrt{2}[\Phi_1^{(1)} - \Phi_1^{(2)}]$ (core state Δ_2') or $\frac{1}{2}\sqrt{2}[\Phi_4^{(1)} + \Phi_4^{(2)}]$ (valence state Δ_1) or $\frac{1}{2}\sqrt{2}[\Phi_6^{(1)} - \Phi_6^{(2)}]$ (excited state Δ_2'), as can be seen from the coefficients of Table VI and Fig. 1. Similarly the combination $\frac{1}{2}\sqrt{2}[\Phi_2^{(1)} - \Phi_2^{(2)}]$ (deep valence state Δ_2') decreases the electron density between the two molecules per unit cell in a more effective way than $\frac{1}{2}\sqrt{2}[\Phi_1^{(1)} + \Phi_1^{(2)}]$ (core state Δ_1) or $\frac{1}{2}\sqrt{2}[\Phi_4^{(1)} - \Phi_4^{(2)}]$ (valence state Δ_2') or $\frac{1}{2}\sqrt{2}[\Phi_6^{(1)} + \Phi_6^{(2)}]$ (excited state Δ_1).

We notice, at last, that the lone-pair molecular orbitals that are loosely bound in the molecule give the highest-energy valence states.

On the basis of the band structure of Fig. 4 we can give an interpretation of some features of the optical properties of CI. The experimental data
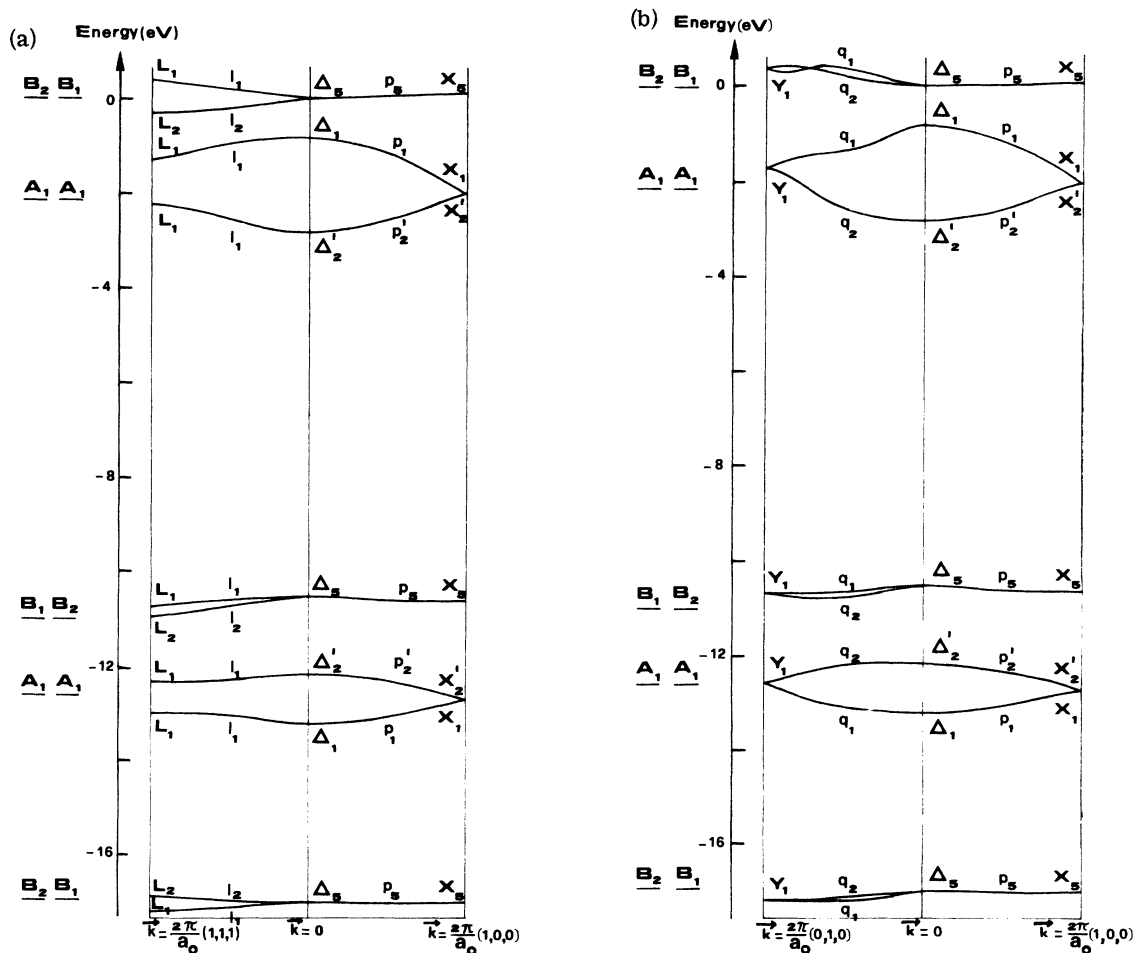
FIG. 4. (a) Valence and excited bands of the cubic-ice model structure at the points Δ, l, L, p, X. For convenience the molecular-orbital energies are also reported. (b) Valence and excited bands of the cubic-ice model structure at the points Δ, p, X, q, Y.

TABLE XI. Values of the energy of the crystal states at the points Δ, X, Y, L. Energies are in eV.

Core states	Δ_2'	−559.40	X_2'	−559.33	Y_1	−559.33	L_1	−559.36
	Δ_1	−559.26	X_1	−559.33			L_1'	−559.29
Deep valence states	Δ_1	−37.33	X_1	−34.99	Y_1	−34.94	L_1	−36.19
	Δ_2'	−32.19	X_2'	−34.99			L_1	−33.63
Valence states	Δ_5	−17.06	X_5	−17.05	Y_1	−17.18	L_1	−17.18
							L_2	−16.91
	Δ_1	−13.20	X_1	−12.70	Y_1	−12.64	L_1	−12.97
	Δ_2'	−12.17	X_2'	−12.70			L_1	−12.33
	Δ_5	−10.58	X_5	−10.60	Y_1	−10.72	L_2	−10.96
							L_1	−10.75
Excited states	Δ_2'	−2.76	X_2'	−1.94	Y_1	−1.71	L_1	−2.29
	Δ_1	−0.84	X_1	−1.94			L_1	−1.28
	Δ_5	0.09	X_5	0.12	Y_1	0.38	L_2	−0.34
							L_1	0.38

of Onaka et al.[4] show a sharp edge in the optical constants at ≈ 8 eV. We interpret this threshold as related to the critical point M_0, due to the transition at 7.8 eV between the Δ_5 valence state and the Δ_2' excited state, which is allowed for light polarized perpendicular to the fourfold axis (Table 5) in our simplified model.[24] This assignment is also supported by the fact that the fundamental absorption shifts to lower energy in water,[4] which is consistent with the fact that the Davydov splitting increases under pressure and shifts the Δ_2' excited state to lower energy.[25]

The experimental data of Onaka[4] show an unresolved absorption band, about 1 eV broad, around 8.7 eV. At the point L of the Brillouin zone, the joint density of states between the two lowest excited bands and the two highest valence bands has two critical points of type M_1 with energies of 8.5 and 8.7 eV, and two critical points of type M_2 with energies of 9.5 and 9.7 eV. We interpret the two critical points M_1 as responsible for the strong peak at 8.7 eV in the far-ultraviolet spectrum.

At higher energies another broad and unresolved absorption band centered around 15 eV has been found by Daniels[5] by means of electron-energy-loss experiments. Transitions occurring from valence bands derived from lone-pair orbitals to excited bands seem responsible for such absorption bands; however, energy-loss experiments of Daniels[5] are not accurate enough to allow at this stage an assignment of the critical points responsible for the absorption, and further experimental study would be desirable. We notice that the use of synchrotron radiation light, already attempted,[7] and the determination of electron momentum distribution by means of inelastic scattering rays[26] are two powerful tools that could be applied for a better understanding of the optical properties of ice in the energy range above 10 eV.

V. CONCLUSIONS

A reasonably simple model crystal structure with translational symmetry is analyzed to interpret the electronic states and the optical transitions in cubic ice. The model, based on the physical circumstance that the electronic cloud in the water molecule does not deviate too much from spherical symmetry, could be extended to treat other hydrogen-bonded molecular crystals. The band structure obtained in this paper has been proved useful for establishing the correspondence between the water molecular orbitals and the ice crystal states, for the determination of the energy gap and for an interpretation of the first absorption bands in the far-ultraviolet spectrum. We think that the band
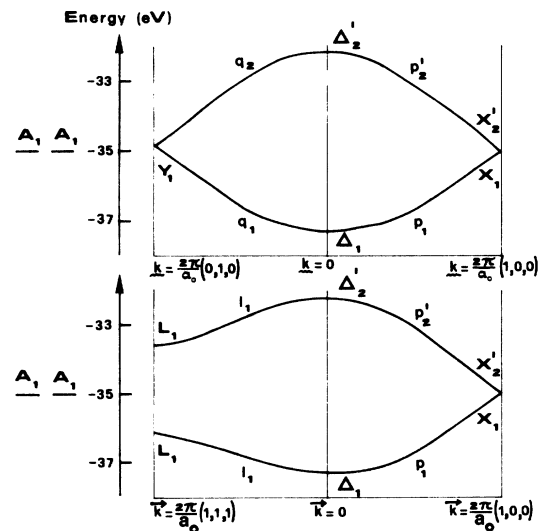
FIG. 5. Deep valence bands of the cubic-ice model structure.

structure obtained will prove useful to interpret and to stimulate the application to ice crystals of widely used and powerful techniques, such as synchrotron-radiation optical properties, inelastic scattering of x rays, and effect of pressure.

ACKNOWLEDGMENTS

APPENDIX A: EXPRESSION OF THE HAMILTONIAN MATRIX ELEMENTS

We assume that the crystal potential $V_c(\vec{r})$ can be written as the sum of water-molecule self-consistent potentials $V_M(\vec{r})$ centered in the appropriate crystal positions, i.e.,

$$V_c(\vec{r}) = \sum_{\vec{\tau}_\nu} \sum_{i''=1,2} V_M^{(i'')}(\vec{r} - \vec{\tau}_\nu) . \tag{A1}$$

We notice that $V_M(\vec{r})$ is not required to be a local operator. The purpose of this appendix is to derive the expression for the Hamiltonian matrix elements (3.12):

$$H_{jj'}^{(ii')}(\vec{k}) = \langle \Phi_j^{(i)}(\vec{k},\vec{r}) | p^2/2m + V_c(\vec{r}) | \Phi_{j'}^{(i')}(\vec{k},\vec{r}) \rangle$$

$$= \sum_{\vec{\tau}_\nu} e^{i\vec{k}\cdot\vec{\tau}_\nu} \langle \psi_j^{(i)}(\vec{r}) | p^2/2m$$

$$+ V_c(\vec{r}) | \psi_{j'}^{(i')}(\vec{r} - \vec{\tau}_\nu) \rangle . \tag{A2}$$

Let us first consider the matrix element

$$\langle \psi_j^{(i)}(\vec{r}) | p^2/2m + V_c(\vec{r}) | \psi_{j'}^{(i')}(\vec{r} - \vec{\tau}_\nu) \rangle \tag{A3}$$

in the case the two molecular orbitals $\psi_j^{(i)}$ and $\psi_{j'}^{(i')}$ are centered on different molecules (i. e.,

either $i \neq i'$ or $\vec{\tau}_\nu' \neq 0$ or both). In the limit of a strong binding,[27] three-center integrals are negligible with respect to two-center integrals and we have

$$\langle \psi_j^{(i)}(\vec{r}) | p^2/2m + V_c(\vec{r}) | \psi_{j'}^{(i')}(\vec{r} - \vec{\tau}_\nu) \rangle$$

$$\approx \langle \psi_j^{(i)}(\vec{r}) | p^2/2m + V_M^{(i)}(\vec{r})$$

$$+ V_M^{(i')}(\vec{r} - \vec{\tau}_\nu) | \psi_{j'}^{(i')}(\vec{r} - \vec{\tau}_\nu) \rangle . \tag{A4}$$

Though the approximation of neglecting three-center integrals is used in most tight-binding calculations, it has become possible to include multicenter integrals if one adopts simple analytic forms for the potential[28] or the discrete variational method by Ellis *et al.*[29] Because of the remarkable computational efforts in extending the above methods[28,29] to molecular crystals and of the fact that the overlap integrals of Table VIII are reasonably small,[30] we have adopted the two-center approximation, summarized in Eq. (A4). We now add and subtract the operator $p^2/2m$ in Eq. (A4), and we obtain

$$\langle \psi_j^{(i)}(\vec{r}) | p^2/2m + V_c(\vec{r}) | \psi_{j'}^{(i')}(\vec{r} - \vec{\tau}_\nu) \rangle$$

$$\approx \langle \psi_j^{(i)}(\vec{r}) | p^2/2m + V_M^{(i)}(\vec{r}) + p^2/2m$$

$$+ V_M^{(i')}(\vec{r} - \vec{\tau}_\nu) - p^2/2m | \psi_{j'}^{(i')}(\vec{r} - \vec{\tau}_\nu) \rangle$$

$$= (E_j + E_{j'}) \langle \psi_j^{(i)}(\vec{r}) | \psi_{j'}^{(i')}(\vec{r} - \vec{\tau}_\nu) \rangle$$

$$- \langle \psi_j^{(i)}(\vec{r}) | p^2/2m | \psi_{j'}^{(i')}(\vec{r} - \vec{\tau}_\nu) \rangle . \tag{A5}$$

Let us now consider the matrix elements of type (A3) when $\vec{\tau}_\nu = 0$ and $i = i'$. We have

$$\langle \psi_j^{(i)}(\vec{r}) | p^2/2m + V_c(\vec{r}) | \psi_{j'}^{(i)}(\vec{r}) \rangle$$

$$= \langle \psi_j^{(i)}(\vec{r}) | p^2/2m + V_M^{(i)}(\vec{r}) + V_c'(\vec{r}) | \psi_{j'}^{(i)}(\vec{r}) \rangle$$

$$= E_j \delta_{jj'} + \langle \psi_j^{(i)}(\vec{r}) | V_c'(\vec{r}) | \psi_{j'}^{(i)}(\vec{r}) \rangle , \tag{A6}$$

where $V_c'(\vec{r})$ is the sum of the potential of the molecules of the crystal except the molecule (i) in the unit cell. The term

$$\langle \psi_j^{(i)}(\vec{r}) | V_c'(\vec{r}) | \psi_{j'}^{(i)}(\vec{r}) \rangle \tag{A7}$$

corresponds to the crystal field integrals[27] in the case of molecular crystals. To estimate (A7) we have considered the quantity

$$I_{jj'} = \langle \psi_j^{(i)}(\vec{r}) | V_M^{(i'' \neq i)}(\vec{r}) | \psi_{j'}^{(i)}(\vec{r}) \rangle , \tag{A8}$$

which is the most important contribution to (A7). The expression of $I_{jj'}$ is

$$I_{jj'} = \sum_{m,n=1}^{7} a_{jm}^{(1)} a_{j'n}^{(1)} \int \left[- \frac{z_0 e^2}{|\vec{r}_1 - \vec{\delta}_{2O}|} - \frac{e^2}{|\vec{r}_1 - \vec{\delta}_{3H}|} - \frac{e^2}{|\vec{r}_1 - \vec{\delta}_{4H}|} \right] \varphi_m(\vec{r}_1 - \vec{d}_m^{(1)}) \varphi_n(\vec{r}_1 - \vec{d}_n^{(1)}) d\vec{r}_1 \tag{A9}$$

$$+ 2 \sum_{l=1}^{5} \sum_{h,k,m,n=1}^{7} a_{lh}^{(2)} a_{lk}^{(2)} a_{jm}^{(1)} a_{j'n}^{(1)} \iint \frac{e^2}{|\vec{r}_1 - \vec{r}_2|} \varphi_m(\vec{r}_1 - \vec{d}_m^{(1)}) \varphi_n(\vec{r}_1 - \vec{d}_n^{(1)}) \varphi_h(\vec{r}_2 - \vec{d}_h^{(2)}) \varphi_k(\vec{r}_2 - \vec{d}_k^{(2)}) d\vec{r}_1 d\vec{r}_2 \tag{A10}$$

$$- \sum_{l=1}^{5} \sum_{h,k,m,n=1}^{7} a_{lh}^{(2)} a_{lk}^{(2)} a_{jm}^{(1)} a_{j'n}^{(1)} \iint \frac{e^2}{|\vec{r}_1 - \vec{r}_2|} \varphi_n(\vec{r}_1 - \vec{d}_m^{(1)}) \varphi_n(\vec{r}_2 - \vec{d}_n^{(1)}) \varphi_h(\vec{r}_1 - \vec{d}_h^{(2)}) \varphi_k(\vec{r}_2 - \vec{d}_k^{(2)}) d\vec{r}_1 d\vec{r}_2 , \tag{A11}$$

where (A9) is the nuclear-charge Coulomb contribution, (A10) is the electronic Coulomb contribution, and (A11) is the electronic exchange contribution. From (A9)–(A11) and Table VII the matrix $I_{jj'}$ has been evaluated[22] and is reported in Table XII. From Table XII we notice that the diagonal matrix elements are almost equal, while off-diagonal matrix elements are about one order of magnitude smaller. In the case the potential of the molecule centered in i' in the unit cell could be considered constant in the region of the other molecule, $I_{jj'}$ would be proportional to the unit matrix. Since the diagonal matrix elements are almost equal, in discussing electronic transitions we can neglect them because their only effect is a rigid shift of the whole band structure. Equation (A6) thus becomes

$$\langle \psi_j^{(i)}(\vec{r}) | \, p^2/2m + V_c(\vec{r}) \, | \psi_j^{(i)}(\vec{r}) \rangle \approx E_j \delta_{jj'} \ . \qquad (A12)$$

The results (A5) and (A12) can be summarized in the following expression:

$$\langle \psi_j^{(i)}(\vec{r}) | \, p^2/2m + V_c(\vec{r}) \, | \psi_{j'}^{(i')}(\vec{r} - \vec{\tau}_\nu') \rangle$$

$$= (E_j + E_{j'}) \langle \psi_j^{(i)}(\vec{r}) | \, \psi_{j'}^{(i')}(\vec{r} - \vec{\tau}_\nu') \rangle$$

$$- \langle \psi_j^{(i)}(\vec{r}) | \, p^2/2m \, | \psi_{j'}^{(i')}(\vec{r} - \vec{\tau}_\nu') \rangle$$

TABLE XII. Crystal field matrix between two nearest-neighbor molecules. Matrix elements are in rydbergs.

$I_{11} = 0.0394$	$I_{12} = 0.0001$	$I_{13} = 0.0007$	$I_{14} = -0.0003$	$I_{15} = 0$
$I_{21} = 0.0001$	$I_{22} = 0.0402$	$I_{23} = 0.0122$	$I_{24} = -0.0019$	$I_{25} = 0$
$I_{31} = 0.0007$	$I_{32} = 0.0122$	$I_{33} = 0.0394$	$I_{34} = -0.0026$	$I_{35} = 0$
$I_{41} = -0.0003$	$I_{42} = -0.0019$	$I_{43} = -0.0026$	$I_{44} = 0.0359$	$I_{54} = 0$
$I_{51} = 0$	$I_{52} = 0$	$I_{53} = 0$	$I_{45} = 0$	$I_{55} = 0.0377$

$$- \delta_{\vec{\tau}_\nu' 0} \, \delta_{ii'} \, [E_j \delta_{jj'} - \langle \psi_j^{(i)}(\vec{r}) | \, p^2/2m \, | \psi_{j'}^{(i')}(\vec{r}) \rangle] \ . \qquad (A13)$$

Expression (A2) becomes, using (A13),

$$H_{jj'}^{(ii')}(\vec{k}) = \sum_{\vec{\tau}_\nu'} e^{i\vec{k}\cdot\vec{\tau}_\nu'} [(E_j + E_{j'}) \langle \psi_j^{(i)}(\vec{r}) | \, \psi_{j'}^{(i')}(\vec{r} - \vec{\tau}_\nu') \rangle$$

$$- \langle \psi_j^{(i)}(\vec{r}) | \, p^2/2m \, | \psi_{j'}^{(i')}(\vec{r} - \vec{\tau}_\nu') \rangle$$

$$- \delta_{ii'} \, [E_j \delta_{jj'} - \langle \psi_j^{(i)}(\vec{r}) | \, p^2/2m \, | \psi_{j'}^{(i')}(\vec{r}) \rangle] \ . \qquad (A14)$$

Using (3.10) and (3.11) we finally obtain

$$H_{jj'}^{(ii')}(\vec{k}) = (E_j + E_{j'}) S_{jj'}^{(ii')}(\vec{k}) - P_{jj'}^{(ii')}(\vec{k})$$

$$- \delta_{ii'} \, [E_j \delta_{jj'} - \langle \psi_j^{(i)}(\vec{r}) | \, p^2/2m \, | \psi_{j'}^{(i')}(\vec{r}) \rangle] \ . \qquad (A15)$$

*Based on work supported in part by Ente Nazionale Idrocarburi (Italy) through a contract with the University of Rome.

[1]N. H. Fletcher, *The Chemical Physics of Ice* (Cambridge U. P., London, 1970).

[2]D. Eisenberg and W. Kauzmann, *The Structure and Properties of Water* (Clarendon, Oxford, England, 1969).

[3]See, V. M. Zolotaryov, Opt. Spektrosk. **29**, 1125 (1970) [Opt. Spectrosc. **29**, 599 (1970)], and references therein.

[4]R. Onaka and T. Takahashi, J. Phys. Soc. Jap. **24**, 548 (1968); A. P. Minton, J. Phys. Chem. **75**, 1162 (1971).

[5]J. Daniels, Opt. Commun. **3**, 240 (1971).

[6]For details on synchrotron radiation as a light source see, for instance, G. W. Rubloff, Phys. Rev. B **5**, 662 (1972).

[7]Y. Nakai (private communication).

[8]L. Pauling, J. Am. Chem. Soc. **57**, 2680 (1935). See, also C. A. Coulson and D. Eisenberg, Proc. R. Soc. A **291**, 445 (1966); Proc. R. Soc. A **291**, 454 (1966).

[9]See, for instance N. H. Fletcher, Rep. Prog. Phys. **34**, 913 (1972).

[10]G. Pastori Parravicini and L. Resca, J. Phys. C **4**, L301 (1971); G. Pastori Parravicini and L. Resca, in *The Third International Conference on Vacuum Ultraviolet Radiation Physics*, edited by Y. Nakai (The Physical Society of Japan, Tokyo, 1971), 31 p. A 2-2.

[11]O. Dengel, V. Eckener, H. Plitz, and N. Riehl, Phys. Lett. **9**, 291 (1964); G. Cubiotti and R. Geracitano, Phys. Lett. A **24**, 179 (1967).

[12]R. Onaka (private communication).

[13]G. Honjo and K. Shimoaka, Acta Crystallogr. **10**, 710 (1957).

[14]G. F. Koster, Solid State Phys. **5**, 174 (1957).

[15]C. Herring, Phys. Rev. **52**, 361 (1937).

[16]S. Aung, R. M. Pitzer, and S. I. Chan, J. Chem. Phys. **49**, 2071 (1968). We are grateful to Prof. G. P. Arrighini for recalculating the molecular orbitals of water with the minimal set parameters of S. Aung *et al.*, and for giving us the data of Table VI not contained in the article of S. Aung *et al*.

[17]G. P. Arrighini, C. Guidotti, and O. Salvetti, J. Chem. Phys. **52**, 1037 (1970). We are grateful to Prof. G. P. Arrighini for letting us know his new results on the water molecular orbitals prior to publication.

[18]For reasons of clarity, throughout this paper we will call unoccupied bands (or unoccupied states) of ice with the name "excited bands" (or "excited states") and not with the name "conduction bands" (or "conduction states"). Were we interested in the behavior of an extra electron in the crystal, i.e., in the conduction bands of ice, we would neglect in E_6 and E_7 the exchange and Coulomb interaction of the excited orbital with the hole left in the molecule. This would increase the values of E_6 and E_7 by + 1.378 and 1.477 Ry, respectively (see Refs. 16 and 17), which are quite large quantities. Of course, the determination of conduction bands would also require appropriate recalculation of the expansion coefficients of Table VI.

[19]A. I. Gubanov and A. A. Nran'yan, Fiz. Tverd. Tela **1**, 1044 (1959) [Sov. Phys.-Solid State **1**, 956 (1959)]; C. A. Coulson, L. B. Redei, and D. Stocker, Proc. R. Soc. A **270**, 357 (1962); F. Bassani, in *Semiconductors and Semimetals*, edited by R. K. Willardson and A. C. Beer (Academic, New York, 1966), Vol. 1, p. 21; V. P. Tsvetkov and N. D. Savchenko, Metallofizika (Kiev) **37**, 49 (1971).

[20]J. C. Slater and G. F. Koster, Phys. Rev. **94**, 1498 (1954).

[21]F. M. Mueller, Phys. Rev. **153**, 659 (1967).

[22]We are grateful to Dr. R. Resta for his calculation of the overlap matrix, kinetic-energy matrix, crystal-field matrix, and Hamiltonian matrix among the molecular orbitals of two nearest-neighbor molecules in the three different relative orientations. In particular we are indebted to Dr. R. Resta for the data of Table XII.

[23]A. S. Davydov, *Theory of Molecular Excitons* (McGraw-Hill, New York, 1962).

[24]We note that the selection rules of Table V apply to CIMS. To

study optical transitions in the dipole approximation in the case of cubic ice with statistical disorder, we must replace the modulus square of the matrix element of $\vec{e} \cdot \vec{r}$ between molecular Bloch sums with its average on the solid angle. The selection rules of Table V would have direct application only in the case of a ferroelectric phase of cubic ice.

[25]L. Resca (unpublished).

[26]For a review on this subject see, for instance, M. Cooper, Adv. Phys. **20**, 453 (1971).

[27]See, for instance, G. C. Fletcher, *Electron Band Theory of Solids* (North Holland, Amsterdam, 1971); F. Bassani and G. P. Parravicini, *Electronic States and Optical Properties of Crystals* (Pergamon, Oxford, England, to be published).

[28]E. E. Lafon and C. C. Lin, Phys. Rev. **152**, 579 (1966); R. C. Chaney, C. C. Lin, and E. E. Lafon, Phys. Rev. B **3**, 459 (1971).

[29]D. E. Ellis and G. S. Painter, Phys. Rev. B **2**, 2887 (1970).

[30]See, for instance, a comparison of the band structure of graphite calculated with inclusion of multicenter integrals by G. S. Painter and E. D. Ellis [Phys. Rev. B **1**, 4747 (1970)] with the previous works of F. Bassani and G. Pastori Parravicini [Nuovo Cimento B **50**, 95 (1967)] and E. Doni and G. Pastori Parravicini [Nuovo Cimento B **64**, 117 (1969)] which neglect multicenter integrals. Since in ice the overlap integrals (Table VIII) are smaller than the corresponding integrals for graphite, our neglecting multicenter integrals does not affect the basic band structure features also in the case of ice.